Rev. Adv. Mater. Sci. 40 (2015) 188-207

ZIRCONIA AND CERIA BASED CERAMICS AND NANOCERAMICS – A REVIEW ON ELECTROCHEMICAL AND MECHANICAL PROPERTIES

N.N. Novik[1,2], V.G. Konakov[1,2] and I. Yu. Archakov[1,3]

[1]Research Laboratory for Mechanics of New Nanomaterials, St. Petersburg State Polytechnical University, St. Petersburg 195251, Russia
[2]Insitute of Chemistry, St. Petersburg State University, St. Petersburg 198504, Russia
[3]Institute of Problems of Mechanical Engineering, Russian Academy of Sciences, Bolshoj 61, Vasilievskii Ostrov, St. Petersburg 199178, Russia

Received: November 26, 2014

Abstract. Zirconia (ZrO_2) and ceria (CeO_2) based ceramics is widely applied in electrochemical devices due to its high ionic conductivity coupled with high mechanical properties. Nowadays, the task of the decrease in the working temperature of such devices is of current interest, there are a lot of papers dealing with this problem. The present paper considers the conductivity vs composition dependencies for such ceramics, it is shown that triple systems are very perspective compositions, especially with hafnium oxide additions. The effect of ceramics microstructure on the conductivity is discussed, in particular the dependence of the grain size on the electrochemical properties, a special attention is paid to nanosized ceramics. Experimental results obtained in this field are compared with those computed using BLM model for microsized case and n-GCM model for nanosized one. The data on the grain size effect on the ceramics mechanical properties are summarized, it is shown that the decrease in the grain size usually results in the ceramics hardening.

1. INTRODUCTION

Zirconia and ceria based solid solutions are widely applied in industry as solid electrolytes for fuel cells [1-3] and electrochemical sensors [4] due to the high ionic conductivity of these materials. At the same time, it is possible to use them in the exploitation regimes under the conditions that eliminate electronic conductivity harmful for fuel cells and electrochemical sensors application. The conventional temperature range for the above materials is 1000 – 1200 °C, however, most of solid oxide fuel cell (SOFC) advantages - the use of non-hydrogen fuels and non-platinum catalysts can be achieved at lower temperatures of 600-800 °C. However, the membrane conductivity in this temperature range is insufficient for the effective SOFC work and it is necessary to increase the working temperature up to 1000-1200 °C to achieve reasonable membrane conductivity values. Since the work at such a high temperatures requires complex technical decisions and needs the application of refractory materials, the task of the SOFC working temperature decrease is very actual, because it will result in significant simplification in the devise construction and increase in their cost efficiency.

One of the possible decisions of this problem is to increase the conductivity of zirconia- and ceria-based materials by their doping as well as by the

Corresponding author: V.G. Konakov, e-mail: vgkonakov@yandex.ru

grain size decrease down to nanoscale region [5]. In order to formulate the approach for this task, the clear understanding of the conducting mechanism structure and the peculiarities of the application of the conventional zirconia and ceria materials is necessary. This paper reviews three major factors determining the oxide ceramics conductivity:
(1) The composition of zirconia- and ceria-based solid solutions and the dopant content in them;
(2) The structure of the polycrystalline electrolyte;
(3) The particle size of the initial precursor powders and the grain size in the electrolytes (final ceramics).

In addition, some general information on the solid electrolytes conductivity will be considered. It should be noted that this review deals with bulk ceramics; data on thin films which are also widely used in a wide range of electrochemical devices can be found elsewhere, see, e.g. [6].

2. SOLID ELECTROLYTES CONUCTIVITY

Perfect ion crystals based on oxide systems do not possess electroconductivity. Ion transitions (ionic conductivity) in solid crystalline electrolytes are possible due to the existence of the crystal lattice defects. These defects could be subdivided into three groups:
(1) Point defects, i.e. defects in the crystal structure with the size comparable to interatomoc distance;
2) Linear defects (dislocations) which are typically characterized by a shift of the periodic structure in some direction;
(3) Planar defects including stacking faults as well as inner and outer surfaces.

Point defects provide the transport properties of solid electrolytes, i.e. their ionic conductivity. According to one of the mechanisms (Frenkel's disordering mechanism), disordering appears due to the fact that a number of atoms is transferred into the interstices with the simultaneous formation of the same number of vacancies. This mechanism, in particular, can be realized due some thermal fluctuations. Another mechanism (Schottky disordering) assumes the formation of the equal number of anion and cation vacancies. At that, the corresponding ions move to the crystal surface.

Frenkel's defects are typical for pure metal oxides considered in this review [7]. Electricity transfer in a solid electrolyte with oxygen vacancies is due to the defects which formation can be described within the frames of Kröger-Vink notation (used here and below) by the reaction

$$O_0 \rightarrow O_i'' + V\ddot{o}. \quad (1)$$

Note that the complete ionization is assumed here, i.e. electrons are absent on the outer electron shell of the atom. According to thermodynamics, the reaction constant here is

$$K_1 = [V\ddot{o}][O_i''], \quad (1a)$$

where [Vö] is the oxygen vacancies content and $[O_i'']$ - is the oxygen content in the intercites.

Depending on the oxygen partial pressure, zirconia and ceria could be both oxygen depleted or oxygen enriched oxides, the equation for oxygen balance here can be written as:

$$O_0 \rightarrow 1/2\,O_2 + V\ddot{o} + 2e^-, \quad (2)$$

$$K_2 = [V\ddot{o}]n^2 p_{O_2}^{1/2}, \quad (2a)$$

where n is the electron concentration and p_{O2} is the oxygen partial pressure. To perform the complete mathematical description, the equation for the holes/electrons balance should be added:

$$O \rightarrow e' + h^{\cdot} \quad (3)$$

with the equilibrium constant

$$K_3 = np. \quad (3a)$$

where p is the hole concentration.

The total current density is

$$I = \sigma E, \quad (4)$$

where σ is the conductivity and E is the intensity of the electric field in which these particles are moving.

The current density due to charged particles transfer will be equal to:

$$I_i = \sigma_i E, \quad (5)$$

where σ_i is the conductivity of consistuent "*I*".

When both electronic and ionic conductivity are present, the total electroconductivity is given by their sum. For the single ion type, it can be written as:

$$\sigma = \sigma_{ion} + \sigma_{el} = \sigma\left(t_{ion} + t_{el}\right), \quad (6)$$

where σ_{ion} and σ_{el} – the inputs of ionic and electronic conductivities and t_{ion} and t_{el} are ion and electron transport numbers. It is known that

$$I_i = c_i q_i u_i = c_i z_i e u_i, \quad (7)$$

where z_i is the valence, c_i – particle content, u_i-particle mobility, and q_i – particle charge.

Basing on the above equations, three types of the dependencies of the vacation concentration and conductivity on the oxygen partial pressure can be considered for zirconia and ceria. In case of stoichiometry

$$[\text{Vö}] = [\text{O}_i''] = K_1^{1/2}.$$

The vacancy content here is independent from the partial oxygen pressure.

The input of n-type electronic conductivity, i.e. the conductivity caused by electron transfer, is rather high at low values of the oxygen partial pressure.

If $[\text{Vö}] = 1/2n >> [\text{O}_i'']$, then

$$n = (2K_2)^{1/3} p_{\text{O}_2}^{-1/6}, \quad (8)$$

$$\sigma = e\left(u_{\text{ion}} + u_{\text{el}}\right)\left(2K_2\right)^{1/3} p_{\text{O}_2}^{-1/6}. \quad (9)$$

As a result

$$\sigma \sim p_{\text{O}_2}^{-1/6}.$$

p-type conductivity, i.e. hole conductivity, usually manifests itself at high oxygen partial pressures.

If $[\text{O}_i''] = 1/2p >> [\text{Vö}]$, then

$$1/2\,\text{O}_2 \rightarrow \text{O}_i'' + 2\,\text{h}^{\cdot}, \quad (10)$$

$$K_4 = [\text{O}_i'']p^2 p_{\text{O}_2}^{1/2}, \quad (11)$$

$$p = 2\left(K_4/4\right)^{1/3} p_{\text{O}_2}^{1/6}. \quad (12)$$

As a result

$$p \sim p_{\text{O}_2}^{1/6},$$

Accounting for Eq. (6) and with regard to the fact that electronic conductivity prevails at the high oxygen partial pressures, one can conclude that

$$\sigma \sim p_{\text{O}_2}^{1/6}.$$

The content of defects in pure zirconia is very low, usually this value is about a few tenths of a percent. It should be also noted that pure zirconia possess monoclinic (baddeleyite) structure at normal conditions [8]. The transition to tetragonal structure takes place at temperatures ~ 1100 °C and the fluorite-like cubic structure forms at 2371 °C with the melting temperature of 2715 °C. Fluorite-like structures are face-centered cubic lattices in which all tetrahedral sites are occupied by the ions; such structures are characterized by high values of ionic conductivity, this is possibly due to the presence of a large number of octahedral voids. Pure ceria possess fluorite-like structure at a room temperature, however, it does not have enough amount of vacancies to provide high ionic conductivity.

The addition of some oxide with a lower cation charge as a dopant gives rise to the significant increase of the oxygen vacancies content. Yttrium oxide (Y_2O_3) is a widely used dopant to zirconia, yttrium stabilized zirconia (a range of ZrO_2-Y_2O_3 system compositions) is usually named as YSZ. Such additions give an opportunity to stabilize favorable for ionic conductivity fluorite-like cubic modification of zirconium oxide. Let us consider the thermodynamics of the ionic conductivity formation using the following case. The process of the vacancy formation can be described by the equation below.

$$\text{Y}_2\text{O}_3 + 2\,\text{Zr}_{\text{Zr}}^{\text{X}} + \text{O}_{\text{O}}^{\text{X}} \rightarrow 2\,\text{Y}_{\text{Zr}}' + \text{Vö} + 2\,\text{ZrO}_2. \quad (13)$$

Consideration of this equilibrium, Eq. (13), should be performed taking into account the electrical neutrality condition. For moderate oxygen partial pressures, it can be with a sufficient precision written as:

$$2[\text{Vö}] = [\text{Y}_{\text{Zr}}'], \quad (14)$$

Thus, the amount of oxygen vacations is determined by the dopant content. The exact form of the electrical neutrality equation is:

$$p + 2[\text{Vö}] = n + [\text{Y}_{\text{Zr}}'] + 2[\text{O}_i'']. \quad (15)$$

The temperature dependence of the electrolyte conductivity can be expressed by Arrhenius equation.

$$\sigma = \sigma_0 \exp\frac{-E_A}{kT}, \quad (16)$$

where σ_0 is the preexponential factor, E_A is conductivity activation energy, T is the absolute temperature, and κ is the Boltzmann constant.

Dopants existence provide to possibility for the significant change in the defect content. Doping ions often form a wide range of solid solutions with the basic component, this means that the doping ions are completely integrated in the crystal lattice of the basic component. However, the heterogeneous structure formation due to incomplete dopant solution or the case of the complete dopant insolubility can be also considered, this consideration will be given below. Generally, the existence of solid solutions with dopants having the ion charge both higher and lower than that of the basic component ion is possible. But the conventional practice for zirconia and ceria based materials is the use of the oxides

with the metal valence lower than that of zirconium and cerium. Hence, doubly (Ca and Mg) and triply (Y,Sc,Yb, Sm, Gd, etc.) charged metals are applied, this review will consider these dopants application.

Electronic conductivity, as a rule, is undesirable in most of solid electrolyte applications, the exception is solid electrolytes for fuel cells, the mixed electronic-ionic conductivity is an advantage for them [9]. Note that n-type conductivity is typical for the stabilized zirconia at the oxygen partial pressures lower than 10^{-30} atm.

Summarizing the above consideration, we cab state that ionic conductivity prevails in zirconia and ceria based electrolytes in a wide range of oxygen partial pressures. However, the determination of the conductivity type is necessary for each certain composition, the study of the electrolyte conductivity vs oxygen partial pressure dependence should be carried out for such determination. Doping by different oxides could provide high ionic conductivity. Conventionally used doped electrolytes possess optimal conductivities at rather high temperature, for this reason, the attempt of the alternative dopants application providing the decrease of the working temperature and the increase of the oxygen partial pressure range is a point of essential interest.

3. THE EFFECT OF SYNTHERING APPROACHES AND THE PRECURSOR POWDERS POST TREATMENT PROCEDURES ON THE OXIDE SOLID ELECTROLYTES PROPERTIES

The process of ceramic (including nanoceramic) electrolytes manufacturing is well developed, it includes the following steps.

1) Precursor powders synthesis;
2) Post treatment of the precursor powders (including thermal and mechanical treatment) in order to obtain required particle properties and structure;
3) Precursor powders compactification into the final unit;
4) Thermal treatment of the final units manufactured from solid metal oxide electrolytes (if necessary).

Precursor powders synthesis approaches may affect on such properties of solid electrolytes as grain size, density, uniformity of dopant distribution in a solid solution, etc. At present, a lot of physical and chemical methods are used for this task, solid phase ceramic synthesis and different modifications of sol-gel synthesis are widely used here. Let us consider these two approaches in more detail.

Solid phase synthesis was conventionally used for solid electrolyte manufacturing; the idea of this approach is the calcination of the oxide powders mixture, sometimes pretreatment of the powders (mechanical activation) is applied before the calcinations step. The main advantage of this method is its simplicity; however, small particle size cannot be obtained here. In addition, problems with the uniform components distribution in the final material were reported [10]. Another disadvantage of the method is a necessity of high temperature calcination in order to provide mutual diffusion of the components.

Sol-gel synthesis is widely used nowadays for the task of solid electrolyte manufacturing. This approach provides the uniform distribution of the solid solution components due to their homogeneous distribution in the precursor powders.

The following versions of sol-gel synthesis are usually used:

- partial neutralization of the metal salt with the formation of a stable hydrosol that is the mixture of high-dispersed hydroxides;
- complete neutralization of the metal salt with following washing and precipitate peptization resulting in stable hydrosol formation;
- metal salt hydrolysis at high temperatures;
- metal organic compound hydrolysis.

The process can be generally described by the following steps: initial components homogenization, their conversion into a sol, then into a stable sol, and final drying.

The most important versions of sol-gel approach are alkoxide hydrolysis and reverse precipitation of the metal salts.

The first approach includes water addition to the alcohol solutions of metal and non-metal alkoxides with the general formula $M(OR)_n$ (M = Si, Al, Ti, V, Cr, W, Zr; R = CH_3-, C_2H_5-, C_3H_7-, etc.). This pathway results in hydrolysis with further polycondensation at low temperatures according the following reactions:

$$M(OR)_n + H_2O \rightarrow \left[M(OR)_{n-1}(OH)\right] + ROH, \quad (17)$$

$$M\text{-}OH + M\text{-}OX \rightarrow M\text{-}O\text{-}M + XOH (X=H \text{ or } M). \quad (18)$$

As a result, hydroxilated M-OH groups and hydroxide monomers are formed; they manifest themselves as the active centers in the polycrystallization reaction that likely occurs according to the alkoxylation mechanism.

The reverse copresipitation approach in based on particle precipitation from the solution by a third

component. Usually, aqueous ammonia is used as such a third component. The approach providing the precipitation conditions optimization was reported in [11], the authors of [12] proved the possibility of the nanosized particles production. The obtained gel is purified from undesirable additions and dried. It is known that gel thermal treatment affect the size and morphology of the final particles. Such approaches as drying under pressure and azeotropic drying provide the opportunity to control particle morphology and to decrease the average particle size down to nanoscale region. Decreasing the average particle size, these drying procedures also decrease the mechanical strength of agglomerates; however, their use is associated with significant labor costs. Modern freeze-drying approach is less studied. This method bases on water removal from the gel due to its sublimation at low temperatures. Freeze-drying provides an opportunity to control the particle size and agglomerate structure; however, it requires proper equipment.

Comparing the electroconductivity of YSZ samples manufactured by conventional ceramic method and synthesized by reverse co-precipitation approach, the authors of [13] conclude that the conductivity of ceramics is similar for both production approaches at a same thermal treatment. On the other hand, ceramics produced from the sol-gel powders possesses lower density, this fact can be considered as some additional possibility to increase the conductivity of the ceramics produced by sol-gel approach. The increase in the calcination temperature results in the increase in the ceramic density of the samples synthesized by reverse co-precipitation approach; in turn, this increases its electroconductivity, such an increase is impossible in case of ceramics produced via conventional ceramic approach.

Authors of [14] demonstrated that, under certain conditions, nanocrystalline zirconia could inherit the structure of the initial amorphous xerogels, this fact should be taken into account during the synthesis of nanopowders with required structures. This idea seems to be reasonable, however it is not widely used for today.

Powder compactification method could also affect the ceramics conductivity, in addition, it also affects on such important for electrochemical applications properties as ceramics density and its gas permeability. Most electrochemical devices require ceramics with maximal density and minimal porosity, thus, the increase in the final ceramics density is the principal task. The conventional approach to powders compactification is an isostatic pressing followed by calcination. In doing so, one can produce ceramics with the density up to 97-98% of theoretical density calculated for the ideal ceramics [15-16]. Hot pressing is the perspective approach providing the significant increase in zirconia and ceria based ceramics density. This method was intensively studied in 1980th, the details on the technology could be found in [17], the results of its application are summarized in [18]. One should distinguish usual hot pressing, i.e. simultaneous pressing in two directions during the ceramics calcination from hot isostatic pressing which considers the use of incompact media (in particular, gases) for uniform pressure application in all directions. Regretfully, the works comparing the effect of compactification approach on the ceramics conductivity are practically absent; the comparison of the results of different authors is very difficult due to the impossibility to control all pressing parameters. Let us briefly consider some of a few papers in this field. Masaki et al. [16] compared the structure and mechanical properties of partly stabilized zirconia with yttria content from 1.5 to 5 mol.%. Here and further the composition is given in mole percent unless the other is mentioned. Comparing such approaches as cold isostatic pressing, conventional hot pressing, and hot isostatic pressing, the authors demonstrated that hot isostatic pressing results in the ceramics density close to theoretical limit. At that, the increase in other mechanical properties is registered, for example, the bending stress increases by one-third. To our regret, the data on electroconductivity are not discussed, some conclusions could be done using indirect data. One of the alternative pressing approaches is the electric field application, paper [19] compares ceramics electroconductivity in the samples produced by hot pressing and electric field application. It is concluded that the Arrhenius dependencies and the activation energies values are quite similar for samples manufactured by both approaches. An interesting conclusion is done on the effect of the use of micro- and nanosized precursors on the final ceramics density. The authors claim that the ceramic density higher than 99% of theoretical limit can be obtained only at a final grain size exceeding 1 μm. The problems of dense nanoceramics (ceramics with the nanosized grains) production is mentioned in some other works, see Section 7 below. Arguing with the above concept, we can state that the application of modern compactification approaches coupled with the increase in the thermal treatment temperature provides the possibility to produce dense ceramics with the grain size close to nanosized.

It is known that higher pressure application limits the face growth, for this reason such modern methods as magnetic pulse pressing [20] and spark plasma (HIP) pressing [21] are used to produce dense nanosized ceramics.

The usual requirement for electrochemical devices based on solid oxides (primarily, fuel cells) is the possibility of their exploitation at temperatures higher that 800 °C. Therefore, the careful study of the further calcinations of the already compactificated ceramics is necessary. It is known that such additional heat treatment (at higher temperatures or at greater calcination durations) could both increase and decrease electrical properties of the ceramics. The most critical factor here is the effect of calcination on the grain boundaries structure, this effect will be considered in detail below in the section discussing the dependence of the conductivity on the electrolyte structure.

4. APPROAHES FOR ELECTROCONDUCTIVITY MEASUREMENTS

Let us briefly discuss the approaches for the solid electrolytes conductivity measurements.

Obviously, the method of electroconductivity measurements should provide an opportunity to eliminate the effect of electrode resistance as well as the effect of the electrode/electrolyte boundary resistance. As an alternative, it should be possible to subdivide the input of these resistances. Nowadays, two- or four-point measurements at a direct current (DC), two- or four-point measurements at alternating current (AC), and electrochemical impedance spectroscopy are used. 3-point and multipoint measurements are also mentioned in literature [22], however, the application of these approaches in practice is very limited.

The idea of 2-point measurement is the voltage application to a sample placed between two electrodes and the determination of the sample resistance. DC usage provides the measurements of the conductivity due to the long distance ion migration instead of the losses due to ion oscillations in coordination polyhedral. In addition, DC measurements require simpler equipment. However, DC measurements need reverse electrodes compatible with the solid electrolytes in the system under investigation. When these conditions are not met, the problem of electrode/electrolyte boundary polarization appears, in this case, the boundary works as a capacitor.

Separation of the different sources inputs is impossible in 2-point DC measurements. However, there is the possibility to evaluate the input of interphase resistance measuring the resistance dependence on the electrolyte thickness with further calculations based on the assumptions that polarization resistance does not depend on the electrolyte thickness. More often, 2-point AC measurements at a certain frequency are used, the frequency is selected regarding for ceramic structure and experimental conditions. These measurements are performed using the Wheatstone bridge, see the circuitry in [23]. In theory, AC measurements give the opportunity to separate electronic and ionic conductivities and to obtain some more important information. However, the disadvantage of these measurements at a fixed frequency is the fact that the equivalent electrical circuit of the cell is unknown here, there is no assurance that the measured resistance R and capacity C will be equal to the real resistance and capacity of the sample. Thus, the preliminary study aiming in the frequency choice is necessary.

Application of 4-point methods allows to eliminate the effect of electrodes and heterogeneous boundary resistances, so, there is an opportunity to overcome all disadvantages of 2-point approaches. 4-point measurements are usually performed in a DC regime due to simpler equipment required; in addition, more accurate data could be registered here. Some minimal current passes between two “current” electrodes, while the voltage is measured by two “inner” electrodes. The comparison of 2-point and 4-point measurements was reported in [24], it was shown that the Arrhenius curves obtained in 4-point measurements look like more reasonable. The disadvantage of the 4-point approach is a high sensitivity to a sample shape. Another problem is the difficulty of the determining of the distance between the electrodes in case when the extended electrodes are used instead of point ones, however, some approaches give an opportunity to perform 4-point measurements at different electrode shapes.

4-point approach is an express method and it is widely used to obtain the Arrhenius curves for different materials, but it is impossible to separate the inputs of grains, grain boundaries, and electrodes in a polycrystalline sample using this method. To solve this problem, one should use the impedance spectroscopy as an additional investigation procedure.

Impedance spectroscopy gives the detailed data about the ceramics electroconductivity for the case of solid electrolytes based on complex oxide systems. However, some disadvantages of this approach

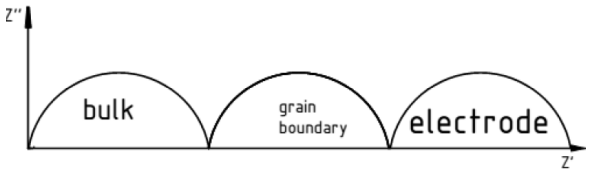

Fig. 1. Typical impedance plot for polycrystalline ceramic.

should be mentioned. Impedance spectroscopy requires more complex and expensive equipment than DC measurements. In addition, AC measurements at a fixed frequency provide more rapid measurement results. The idea of the impedance spectroscopy method is the study of the system reaction on the applied perturbing pulse, this pulse is sinusoidal and possesses low amplitude [25]. There are a number of approaches for the measurements procedure, the following is the most frequently used. AC of a fixed frequency is applied to a sample and the amplitude and the phase shift or the real and imaginary parts of the resulting current are measured. 2-point approach is used here. To describe the electrochemical circuit behavior, the obtained results are compared with those computed for the physical model of the processes occurring in the circuit designed from elementary units having the same reaction on the perturbing pulse [26]. Electrochemical impedance is a vector value, the total system impedance could be presented in the Cartesian coordinate system (Fig. 1) according the following equations.

$$\begin{aligned} Z &= Z' + jZ'', \\ \mathrm{Re}\, Z &= Z' = Z\cos\theta, \\ \mathrm{Im}\, Z &= Z'' = Z\sin\theta. \end{aligned} \qquad (19)$$

Sometime, some characteristics connected with the impedance are measured instead of the impedance itself, the most important among them are:

· Addmitance, which is reciprocal impedance. Addmitance is also called a complex conductivity similarly to conductivity that is a reciprocal resistivity. The combination of impedance and admittance is immittance.

$$\mathrm{Y} = \mathrm{Z}^{-1} = \mathrm{Y}' + j\,\mathrm{Y}'', \qquad (20)$$

· Permittivity, a characterization of the electric induction dependence on the electric field intensity.

$$\xi = \xi' + j\xi''. \qquad (21)$$

· The reciprocal of the permittivity is an electric module

$$\mathrm{M} = 1/\xi = \mathrm{M}' + \mathrm{M}''. \qquad (22)$$

Note that the accurate impedance measurements require thorough elimination of the exterior responses and well as accurate system linearity.

The first works performed in this field were [27] and [28], the latter one considered the separation of the location inputs. The study of solid electrolytes manufactured within different approaches should be mentioned as an essential point of the Baurle works [27]. The study of monocrystals allows to identify the correlation of grain and grain boundary conductivities with the specific regions in the locus plot, see the typical impedance locus and equivalent circuit in Fig. 1 and typical equivalent circuit in Fig. 2

5. SHORT NAMES FOR SOLID SOLUTIONS

The complete list of all solid solution components along with its composition is rather cumbersome, sometimes it hinders the information perception. To avoid this problem, the short names system for solid solutions based on zirconia and ceria was suggested, at present, it is in a general use. It provides the exact description of the solid solution composition as well, as its structure. Generally, some abbreviations are used; let us consider them in part dealing with zirconia modifications used in electrochemical devices.

Stabilized cubic solid solution is the most frequently used substance, it is marked as SZ (stabilized zirconia) with the indication of the stabilizing element in front, e.g. YSZ – yttrium stabilized zirconia. Abbreviation TZP (tetragonal zirconia polycrystals) is used to denote zirconia based solid solutions in the tetragonal modification, the example of such a system is $97ZrO_2$-$3Y_2O_3$ composition. The third type of zirconia based ceramics applied in the electrochemical devices is partly stabilized zirconia which contains cubic phase ZrO_2 (c-ZrO_2) with tetragonal t-ZrO_2 additions, it is denoted as PSZ. The name of the doping element according to periodic table is placed before the abbreviation describing the zirconia structure. There is no necessity to consider such a wide range of structure variations for ceria based polycrystalline systems, the general abbreviation used here is DC (doped ceria). Note that doping elements in this case are denoted us-

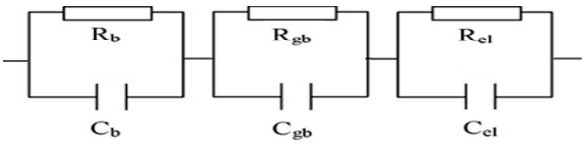

Fig. 2. Equivalent circuit for polycrystalline ceramic.

Table 1. Short names used to denote zirconia and ceria based systems.

Oxide system	Short name
ZrO_2-Y_2O_3 (cubic modification)	YSZ
ZrO_2-Y_2O_3 (tetragonal modification)	YTPZ
ZrO_2-Sc_2O_3	ScSZ
ZrO_2-CaO	CaSZ
ZrO_2-Yb_2O_3	YbSZ
CeO_2-Sm_2O_3	SDC
CeO_2-Gd_2O_3	GDC

ing the first letter in their name (e.g., Y for yttrium) instead of the complete element name, see Table 1.

In order to specify the dopant content, the proper numeral is added in front of the abbreviation (e.g. 8YSZ denoted 92%ZrO_2-8%Y_2O_3 composition). Table 1 lists the abbreviations widely used for zirconia and ceria based systems.

6. THE EFFECT OF SOLID ELECTROLYTE COMPOSITION ON ITS IONIC CONDUCTIVITY

It was Nernst's idea to apply electrical conductivity of zirconia-based materials in practice [29], the attempt to use 15YSZ composition for light bulbs production was performed. In the future, YSZ system has become the basis of electrochemical devices due to reasonable conductivity at high temperature, easy sintering, and relatively low cost. It is well known that maximal YSZ system ionic composition is obtained at minimal content of the doping element necessary for system stabilization [30]. Note that such stabilization is the prerequisite providing ionic conductivity. 8% of the dopant was shown to be such a minimal yttrium content in YSZ system. The decrease in the ionic conductivity at higher dopant concentrations is due to oxygen vacations and dopant ions association in some low-mobile complexes. The mechanism of such association can be written as [31]:

$$Y'_{Zr} + V\ddot{o} \rightarrow \left(Y'_{Zr} V\ddot{o}\right)^{\cdot}. \qquad (23)$$

Note that nanoscaled YSZ under some specific conditions could possess protonic conductivity (the discussion on the application of the term "nanoscaled" to the oxide solid solutions will be given below). Basically, protonic conductivity manifests itself when YSZ material is placed into some wet atmosphere [32], [33], the result is the significant increase in the sample conductivity in contrast to the values typical for non-hydrated samples. Indeed, proton mobility exceeds the mobility of oxygen ions. Guo et al. [34] suggested the following mechanism for this type of conductivity:

$$H_2O + V\ddot{o} + O_O^x \rightarrow 2(OH)_O^{\cdot}, \qquad (24)$$

At the same time, theoretical computations performed within Atomic Simulation approach [34] showed that the proton transport mechanism is primarily associated with the grain boundary conductivity, while the input of the bulk conductivity is low. This is due to the fact that the hydratation energy of grain boundaries is significantly lower than that for grains, for this reason, the proton concentration here is high. This statement is partly proved by the data on thermogravimetry of hydrated zirconia samples and their grain boundary conductivities [33].

8YSZ and 10YSZ degradation at calcination is described in [35]. XRD and neutron diffraction results for calcined samples were compared with those for non-calcined ones in order to study this degradation. It was shown that the ionic conductivity nearly halved after 700 hour calcination. At further calcination, this effect is not so significant. The authors of [35] considers these ionic conductivity behavior as being due to the changes in the vacancy structures and variations in the ion nearest environment.

Goldschmidt's rule is usually used in the case of other dopant application. This rule states that the complete isomorphism is possible only for the atoms with the radii difference lower than 10-15% [36]. It should be noted that the above statement is still under discussion. The authors of [37] suggested the alternative approach - to compare the cubic lattice parameter *a* of the base oxide with the same parameter of the pseudo-cubic lattice of the doping oxide.

For a long time, calcium oxide was used as a basic dopant [38], it was widely used in 1970th. However, stabilization into cubic fluorite-like structure using calcium oxide faces a number of problems. For this reason, nowadays ZrO_2-CaO system is used as a model system only [39] in order to test new synthesis approaches; it is not used now in the electrochemical devices. Similarly, the use of magnesium oxide (MgO) is also ineffective [40] due to the problematic stabilization into cubic fluorite-like structure with divalent alkali-earth cation.

As seen from Table 2, scandium oxide can be considered as one of the effective dopants for zirco-

Table 2. Ionic radii for some metal ions according to Ahrens.

Oxide	Ionic radius of the metal ion, nm
ZrO_2	0.072
HfO_2	0.078
CeO_2	0.053
CaO	0.099
MgO	0.066
Y_2O_3	0.092
Sc_2O_3	0.081
Yb_2O_3	0.086
In_2O_3	0.081
Sm_2O_3	0.100
Gd_2O_3	0.097
Al_2O_3	0.051
Er_2O_3	0.089
Nd_2O_3	0.104
Dy_2O_3	0.092

nia compositions. The conductivity of 8ScSz was studied in [41]. It was shown that cubic structure in ScSZ system is stabilized at dopant content of ~9% [42], while well-ordered β-phase $Sc_2Zr_2O_{17}$ is formed at a dopant content of 11-13%. Synthesis conditions as well as precursor and final ceramics treatment strongly affects phase composition in the system. The authors of [43] reported that the optimal conductivity in the system is reached at ~ 9.3% of Sc_2O_3. The hysteresis on the Arrhenius plot was found for the solid solutions with the scandium oxide content higher than 10% at 500-600 °C, it is considered as being due to the b-phase transition into the cubic phase. On the other hand, such a transition does not produce significant changes in the sample volume, [44] estimated this change as less than 0.15%. So, one can conclude that this phase transition does not lead to intensive ceramic samples destruction, for this reason, cubic phase stabilization is not necessary for the electrolyte application in electrochemical devices.

It should be noted that the application of ZrO_2-Sc_2O_3 solid electrolytes is restricted by the significant degradation of the compositions with low dopant concentration (< 9%) at long lasting calcination or high temperature exploitation. But the high cost of scandium oxide is a reason to use ZrO_2-Sc_2O_3 solid electrolytes with low scandium oxide content in spite of the fact that these compositions are not optimal regarding for their conductivity. There is no common explanation of the above mentioned degradation mechanism, segregation of the doping oxide along with the cubic phase stabilization or the well-ordered phase formation were considered as such mechanisms . The problem of thermal degradation of ScSZ is discussed in detail in [44,45]. Summarizing the existing data, we can state that the practical use of zirconia doped by scandium oxide compositions with the dopant content less than 9% is impossible.

ZrO_2-Yb_2O_3 system does not have this disadvantage [45]. The optimal dopant content here is 8%. The conductivity of 8YbSZ sample decreases by 0.1 S/cm after the 2000 hour calcination at 1000 °C, while no conductivity change was registered for 10YbSZ composition even for 6000 hour calcination at the same temperature. However, the industrial use of YbSZ is limited due to the high cost of ytterbium oxide.

Indium oxide can be treated as a very perspective dopant since its ionic radius is quite similar to that for scandium oxide (see Table 2). Some compositions of ZrO_2-In_2O_3 system were investigated in [46-47]. It was shown that this system is characterized by complex phase composition and a significant number of phase transitions. Cubic fluorite-like solid solutions are formed at indium oxide content in the range from 23.5 to 50%, tetragonal phase is formed at lower dopant content. Maximal conductivity was registered for the composition with 25% of the dopant, this composition is also characterized by maximal activation energy.

Pure ceria possesses fluorite-like structure. Samarium and gadolinium oxides, Sm_2O_3 and Gd_2O_3, respectively, are usually used as the dopants for ceria [48]. The ionic conductivity of ceria solid electrolytes at a dopant content of 10% is 2×10^{-2} S/cm in case of samarium oxide and 5.4×10^{-2} S/cm for Gd_2O_3.

The general problem for ceria solid electrolyte application is the partial reduction of Ce^{4+} to Ce^{3+} [11,30] in the reduction ambience. In particular, such conditions are typical for the fuel cell anode, sometimes they are also possible at chemical sensors exploitation. Such a transition gives rise to a number of problems due to the n-type electronic conductivity that negatively affects electrochemical devices. An addition, possible deviations from stoichiometry and lattice expansion could cause material embrittlement and be a reason of sample destruction. The reaction of such transition following [49] can be written as:

$$2\,Ce_{Ce} + O_O^x \rightarrow V\ddot{o} + 2\,O_2(g) + 2\,Ce'_{Ce}\,. \qquad (25)$$

According to [48], an increase in rare-earth element content facilitates $Ce^{4+} \rightarrow Ce^{3+}$ transition.

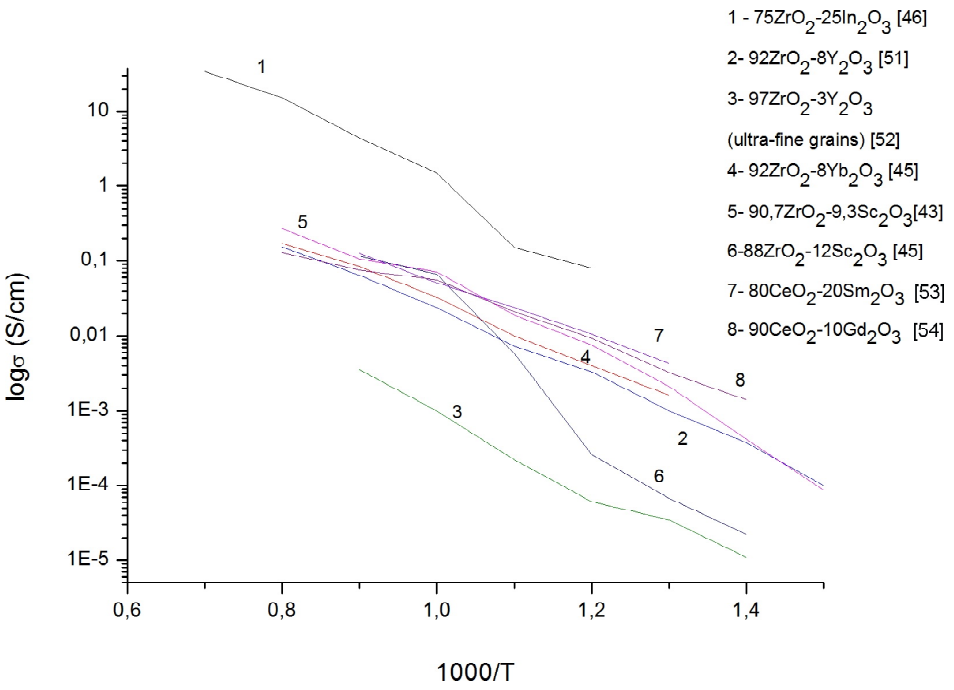

Fig. 3. Ionic conductivity of some binary oxide systems.

The application of yttrium oxide as a stabilizing dopant for ceria is not widely used since the ionic radii difference is rather high here (see Table 2). Correlations between the electrolyte conductivity and YDC ceramics composition are discussed in [50], the maximal conductivity was registered for the sample with 10% of yttria, it equals 4 10^{-3} S/cm at 500 °C. Summary of Arhenious plots obtained for different binary systems is represented in Fig. 3.

At present, triple systems attract increasing interest. Most studies consider YSZ system as a base for such triple system, the point of study is the third component addition. A lot of such dopants are the perspective candidates for the solid electrolytes with improved characteristics, metals usage providing cermets instead of ceramics is very interesting here. Generally, triple systems can be subdivided into two groups: electrolytes based on solid solutions (the case discussed above) and heterogeneous systems that may also possess high ionic conductivity values. For this reason, triple systems compositions providing solid solutions or heterogeneous phase should be the point of essential interest.

Partial replacement of zirconia to hafnia is very perspective. It is well known [55] that zirconia and hafnia have similar structures. Hafnium is isovalent with zirconium, so, hafnia addition to zirconia does not increase the vacancy amount. Actually, hafnia added to zirconia will become the basis of the lattice, i.e., will play the same role as zirconia.

Let us discuss zirconia-hafnia-yttria triple system in more detail. Like zirconia, pure hafnia exists in three forms. Monoclinic form is stable in a wide temperature range from room temperature up to 1800 °C, at this temperature it turns into tetragonal modification. The t → c transition occurs at temperatures between 2500 and 2700 °C. Hafnia melting point is estimated as lying in the temperature range from 2800 to 2850 °C. Comparing these data with zirconia characteristics, one can conclude that hafnia is more stable to temperature than zirconia. The overview of binary ZrO_2-HfO_2 [56] and HfO_2-Y_2O_3 [57] systems is useful to understand changes in triple ZrO_2-HfO_2-Y_2O_3 system structure. It was shown that the cubic fluorite-like structure is stabilized only at 20% of yttria in the binary HfO_2-Y_2O_3 system [56]. It is also known, that the use of nanosized precursors is the only way to get cubic structure in binary ZrO_2-HfO_2 system [58]. The conductivity of binary HfO_2-Y_2O_3, HfO_2-Yb_2O_3, and HfO_2-Sm_2O_3 systems was investigated in [59]. Phase composition of triple ZrO_2-HfO_2-Y_2O_3 system was considered in detail both for zirconia and hafnia enriched regions [60], regretfully, the data are available for a limited set of temperatures. It should be noted that the stable cubic structure was observed for 85%ZrO_2-15%HfO_2 sample doped by Y_2O_3. At 1300 °C, the cubic structure was stable at yttria content from 7.5 to 45%, while at 1600 °C this range was from 8 to 39% of Y_2O_3. The use of nanosized precursors for the synthesis of triple system with hafnia content from 5 to 15% and the effect of nanoscale powders on the final ceramic structure was investigated in [61,62]. The conductivity of nanosized ceramics was mea-

sured by the authors of [62]. Comparing the conductivity of binary YSZ electrolyte with the triple system sample containing 5% of hafnia, the authors of [62] showed that the ionic conductivity of triple system sample at 1000 °C is ~10^{-4} S/cm, this value is two order of magnitude lower than that of pure 8YSZ at the same temperature. The higher is the hafnia content in the triple system, the higher is the ionic conductivity. Authors suggested monoclinic hafnia film formation on the sample surface to be the factor that prevents crystal growth and blocks the ionic transport. In turn, an increase in hafnia content is a reason of blocking effect weakening. This assumption can be supported by the fact that the conductivity of triple system sample with 20% of hafnia is quite similar to that measured for 10YSZ sample [63], i.e. the hafnia content increase eliminate the above discussed losses in conductivity. All authors agreed that conductivity of solid solutions with hafnia addition is less dependent from thermal treatment history. Moreover, triple system has lower electronic conductivity at low oxygen pressure (below 10^{-13} Pa) than binary YSZ samples; this characteristic is good for fuel cells and electrochemical sensors.

Another oxide with a metal isovalent to zirconium in zirconia is titania (TiO_2). Comparing to hafnium, titania possesses low solubility in zirconia due to significant difference in crystal structure. TiO_2 has a rutile structure. Hardening of zirconia based materials is considered as the most expected effect of titania addition to zirconia and YSZ. Another expected effect is an increase in electronic conductivity, that suggestion was confirmed in [64-65] for YSZ with 5% addition of titania. Authors of [66] investigated titania solubility mechanism in 12YSZ. It was shown that TiO_2 addition up to 12% leads to the lattice parameter *a* decrease; it is due to the fact that titanium ions with ionic radii lower than zirconium ones (see Table 2) replace zirconium ions in the crystal lattice according the reaction

$$TiO_2 \rightarrow Ti_{Zr} + 2O_O^X, \quad (26)$$

instead of interstitial dissolution mechanism

$$TiO_2 \rightarrow Ti_{Zr}^{4+} + 2O_2(g) + 4e. \quad (27)$$

Further increase of titania content does not affect lattice parameter, therefore, second phase formation takes place.

Paper [67] discusses the investigation of phase transitions in 2YSZ system with titania addition (from 2 to 60%). Tetragonal and monoclinic solid solution formation are reported at titania content up to 15%, this formation leads to the ionic conductivity mechanism appearance. Mixed electronic and ionic conductivity are present in case of $ZrTiO_4$ formation that takes place at titania content from 40 to 50%.

Triple ZrO_2-CeO_2-Y_2O_3 system is also interesting [11]. The conductivity of this system has mixed mechanism at 800 °C and oxygen pressure range from 1 to 10^{-18} atm. The value of the triple samples conductivity is lower than that for YSZ samples [68].

Addition of 4 at.% and 10 at.% of Mn to YSZ was investigated in [69] and [70], respectively. The transport numbers of ~ 0.99 was reported for 4 at.%Mn ceramics in p_{O_2} region from 10^{-15} to 10^5 Pa. It was shown that ionic conductivity prevails at the same oxygen partial pressures in case of 10 at.%Mn samples; p_{O_2} increase results in the conductivity decrease.

ZnO can be also treated as a possible dopant to YSZ . Addition of zinc oxide to YSZ matrix with the dopant concentration from 0.5 to 10% was investigated in [71]. The samples were sintered at 1300 °C for 2 hours. According to XRD data, cubic fluorite-like solid solutions were formed in all studied samples. ZnO addition positively affects various zirconia properties. For example, the addition of 5% of zinc oxide results in the ceramic density increase up to 96% at cold pressing against 89% for undoped system. Also it leads to significant decrease in grain boundary conductivity that was confirmed by impedance measurements at 300 °C. Probably, it is due to oxide interaction with SiO_2 impurities, see next section for detail. Total conductivity of the ceramics also increases at a small dopant addition. Maximal conductivity was observed at 0.5% of ZnO, it equals 2.89 10^{-2} S/cm against 1.31 10^{-2} S/cm in pure YSZ (data for 800 °C). Authors explain this increase as being due to an increase in the vacancy amount, however, further ZnO addition leads to vacancy association.

Bi_2O_3 is known as a good ionic conductor, in order to combine the advantages of YSZ and Bi_2O_3, authors of [72] synthesized ZrO_2-Y_2O_3-Bi_2O_3 system samples and studied their conductivity. 21YSZ was chosen as a basic composition for Bi_2O_3-containing compositions. Note that the above YSZ system consideration indicates that this composition is not very perspective for manufacturing of solid electrolytes with high ionic conductivity, the authors of [72] are not explaining this choice. It is reported that Bi_2O_3 addition of 1.5% provides system homogeneity. It should be mentioned that the sintering temperature for the samples of the discussed triple system was rather low (~1200 °C), this is due to rela-

tively low melting point of bismuth oxide. TEM analysis was performed to investigate grain boundaries, it was shown that these boundaries are enriched by bismuth oxide. Regretfully, the data on conductivity of bismuth oxide containing YSZ reported in [72] should be carefully checked since they are quite similar to that obtained for binary 21YSZ, the agreement is up to three decimal places.

The use of heterogeneous systems instead of solid solutions, i.e. the use of composite materials, is another way to increase solid electrolytes conductivity. Within such approach, alumina is the most common addition to YSZ. Solubility of Al_2O_3 in zirconia is fairly low. According to [73], alumina solubility in 8YSZ is about 0.5-0.8% depending on sintering condition. The effect of this addition is contradictory.

Authors of [73] report that alumina addition within solubility limit increases the grain boundary resistance due to space-charge effect and decreases this resistance at alumina content exceeding the solubility limit due to the interaction with SiO_2 impurities. Total conductivity slightly increases after the addition of 1% of Al_2O_3 and then decreases due to vacancies association.

Addition of small amount of other oxides to YSZ and CGO is also perspective. Authors of [74] studied the effect of 1.5% Fe_2O_3 addition to YSZ and CGO, paper [75] reports positive results of 0.5% Fe_2O_3 addition to CGO. It was stated that such additions decrease electrolyte sintering temperature and simplify their densification. In addition, grain boundary resistance decreases, this effect is more perceptible for samples containing some impurities. Since the main impurity here is SiO_2, this result can be due to the change of wetting nature of SiO_2 phase. The discussed system behavior is evidently seen in case of CGO since the presence of relatively small amounts of Fe ions that possess smaller size than those of cerium and gadolinium ions increases the ion transport.

Since the synthesis of multicomponent systems is rather complicated, there are only few papers on these objects. $Zr_{0.88}Sc_{0.1}Ce_{0.01}Y_{0.01}O_{1.955}$ synthesized by mechanochemical method is discussed in [76]. This compound has an orthorhombic structure; its conductivity is lower than that of binary ScSZ by the factor of 4. Authors explained this fact by incomplete stabilization of cubic phase and by impurities in raw materials. Addition of 50% of alumna to ZrO_2-HfO_2-Y_2O_3 system is discussed in [63]. Two phase system was obtained, it was reported as being stable. The authors of [63] consider this composition as a perspective one for electrochemical sensors due to the fact that this system combines favorable for electrochemical sensors Nernst dependence typical for ZrO_2-HfO_2-Y_2O_3 with high mechanical properties typical for alumina.

Synthesis of YSZ- and GDC-based composites by solid state method is reported in [77], the extremely low components diffusion is mentioned. Sintering at 1300 °C for 3 days is necessary to provide a slight diffusion resulting in formation of CeO_2 based cubic structure. Since the sintering procedure requires high temperature and long duration, its practical application seems to be ineffective.

7. THE EFFECT OF MICROSTRUCTURE ONE THE IONIC CONDUCTIVITY OF SOLID ELECTROLYTES

Solid electrolytes are polycrystalline materials, for this reason, material microstructure greatly affects their properties. Since nanosized materials are the point of essential interest today, the effect of the grain size on the final ceramics properties is one of the problems of current interest.

The brief review of the conductivity theory presented above is certainly correct for monocrystals . The behavior of monocrystalline YSZ in a wide range of yttria concentration (from 6 to 16%) can be found in [78]. Analyzing the results of this work, one can conclude that there is only one semicircle on impedance curve in case of monocrystalline sample (see Fig. 1 as an example of the impedance curve).

Solid oxide materials synthesized by one of the methods described in Section 3 that are used in real devices are usually polycrystalline materials with different grain orientation. Internal structure of polycrystalline solid electrolytes greatly affects their transport properties. In the case of ceramics, one can consider the conductivity as being due to grains with the conductivity similar to that typical for monocrystals in the temperature range up to 700 °C [79] and due to grain boundaries. Generally, grain boundary ionic transport can proceed both faster than in grain bulk as well as slower, sometimes, the typical values can be some orders of magnitude lower than those for grain conductivity [80]. Thus, grain boundary conductivity could be considered as a critical input to the total conductivity, this statement is evident in case of the grain size decrease leading to the increase in the grain boundary input in the whole structure.

Paper [27] written in 1969 was one of the first works discussing the structure influence on solid

electrolyte conductivity. The comparison of monocrystalline and polycrystalline 10YSZ ceramics was performed, the effect of SiO_2 impurities in the samples was taken into account. The authors of [27] suggested an equivalent circuit for impedance measurements. It was shown that monocryctals have only one semicircle on the impedance curve. Another early work on this point, [28], reported the investigation of grain and grain boundary conductivity for CeO_2-CaO system.

SiO_2 is the main type of impurities concentrated on the grain boundaries, so, it is assumed as a main reason of the decrease in the grain boundary conductivity. The source of silica can be raw materials or additions necessary in the sintering procedure. Sometimes, impurities are considered as an individual phase, this impurity phase can have different properties depending on impurities composition, thermal treatment history, treatment method, and other factors. It was shown in [81] that even 0.2% of SiO_2 can decrease the grain boundary conductivity by the factor of 15. This statement was done for zirconia based electrolytes, however, impurities affect ceria solid solutions in the same way [82]. It is assumed that the decrease in the conductivity is due to thin silica film formation, this fact was proved by TEM and HREM in [83-85]. The effect of silica and alumina content on the 3YTZP impedance was investigated in [83]. It was reported that the increase in SiO_2 content leads to the conductivity decrease, however, system impedance in independent from silica content at high SiO_2 concentration. The authors consider that this effect is due to the fact that maximal film thickness is achieved here. The existence of single silica phase coating all the grain boundaries was also suggested in [81]. In this case, the conductivity, i.e., the ion transport, should be carried out through this phase. However, we should mention that the difference in the grain and grain boundary activation energies is very low [86], this fact contradicts the above speculations.

Basing on the structure investigation, the authors of [87,88] suggested the existence of three types of grain boundaries.

1) “clean” grain boundaries, i.e. grain boundaries without impurity phase formation.

2) grain boundaries containing amorphous phase enriched by impurities especially SiO_2. The phases are usually distributed at triple point, the grain boundary resistivity is significantly increased due to these impurities.

3) Grain boundaries containing crystal oxide (e.g impurities oxide) phase.

At the same time, grain boundary conductivity values in high-purity samples are at least an order of magnitude lower than those registered for grain conductivities [89]. Solute segregation from grains to grain boundaries is the most common explanation for this. Yttria enrichment of grain boundaries in YSZ samples was proved by XPS and AES [90-91]. The effect of segregation was also confirmed by molecular dynamic simulations [92]. It was suggested in [93] that the depletion in oxygen vacancies in the space-charged layers is the main reason of the resistivity increase. The above theoretical approach seems reasonable since the activation energies computed agree well with the experimental data [94].

It was shown in [95] that the mixed blocking mechanism caused both by impurity phases and by segregation is the most common case. According to this paper, the minimal Ca segregation in CaSZ corresponds to a minimum in SiO_2 impurity content.

Since the addition of small amounts of oxide impurities can affect the grain boundary conductivity of solid electrolytes, it is reasonable to discuss alumina and other metal oxides addition considered in the previous section from this point of view. Generally, alumina doping negatively affects conductivity, the optimal alumina content here according to [96] is 2%. Bismuth and iron oxides also decrease the total conductivity [97].

High temperature ceramic sintering is another factor affecting final ceramics conductivity. The effect of YSZ green body sintering at 1350 °C on grain and grain boundary conductivities was studied in [98]. The increase in the sintering time from 1 hour to 4 hours leads to ~3 times rise in the grain boundary conductivity, while the grain conductivity remains unchanged. This is probably due to densification and grain growth in ceramics. We should note that impedance measurement was conducted only at 400 °C, measurements in this temperature range are most sensitive to the grain boundary blocking effect. Ceramics with high SiO_2 content is very sensitive to sintering conditions [99]. GDC grain boundary conductivity increases 4 times due to additional annealing at 1350 °C for 20 hours , various mechanisms can be considered to explain this fact. Most likely, this process is due to segregation of impurities on the grain boundaries. Thermal pretreatment of YSZ before sintering can purify it from silica due to SiO_2 nucleation on YSZ particles surface, [100], the authors of the work report the positive effect of 20 hour pretreatment. High cooling speed after sintering [101] also positively affects the grain bound-

ary conductivity, possibly, it is due to less silica amounts extruded from the bulk to the grain boundary.

Let us briefly consider some mathematics necessary to describe the conductivity process. Full determination of the whole process is rather complicated task, for this reason, some models are usually used. Brick-layer model (BLM) proposed in [102] and named after Burgraaf [103] is a standard approach for microsized ceramics modeling. The main advantages [104] of BLM are good correlation of calculated structural and electrochemical parameters with the experimental data and the opportunity of unambiguous treatment of impedance curve arcs allowing to calculate activation energy, resistance, and other parameters. Grains in this model are roughly considered as cubic-shaped with the edge length d_g, they are divided by grain boundaries with a thickness δ_{gb}. For sample with the length L and cross sectional area A, one will have

$$\sigma_b = L / AR_b, \tag{28}$$

$$\sigma_{gb} = L / AR_{gb}, \tag{29}$$

where R_b and R_{gb} are grain and grain boundary resistance obtained from impedance curve, respectively.

Specific grain boundary conductivity is very important too. It presents the conductivity of the grain boundary region with a thickness of δ_{gb}. The dependence of the specific grain boundary conductivity on the total grain boundary conductivity is expressed by the equation:

$$\sigma_{gb}^{sp} = \frac{\sigma_{gb}^{T} \delta_{gb}}{d_g}. \tag{30}$$

Classic or so called S-BLM brick layer model takes into account serial connection of grains only, hence, some grains do not participate in the computation. SP-BLM [105] is the evolution of the theory which considers both serial and parallel grain connections. Both theories are physically unrealistic in the case of significant grain boundary area, particularly, in case of nanoceramics. The most strict version of the brick-layer model is “Nested cube” model considering 3D-enviroment of atoms, all grain sizes can be described by this model. However, mathematical apparatus of the theory is significantly complicated, the equation cannot be solved analytically here. So, single calculation requires a lot of time and “Nested cube” is inappropriate for trivial calculations. For this reason, we can state that nanosized solid electrolytes conductivity description requires its own models.

8. THE EFFECT OF THE GRAIN SIZE ON CERAMIC CONDUCTIVITY. NANOSIZES CERAMICS

The grain size in the ceramics greatly affects its conductivity, primarily, it is due to the changes in the role of grain boundary at the grain size decrease. Note that there is no standard approach to grain size estimation, different approaches can be found in scientific literature. The most common procedure is the estimation of the average grain size basing on the results of scanning electron microscopy (SEM). However, sometimes crystallite size in case of nanocrystalline precursor powders can be estimated from X-ray diffraction (XRD) data, as well as from the sorption/desorption investigations using the BET theory. Analyzing and comparing the data on the ceramics grain size, one should be very careful since in spite of the above data collected within different approaches are similar and show the same behavior, they are not identical [106,107].

Comparing the effect of grain size on solid electrolytes conductivity, one can conclude that such effects are different for micro- and nanosized electrolytes. Microsized electrolytes were well studied in 1970th, see YSZ studies in [93,108]. It was shown that the integral conductivity of solid electrolytes decreases with the grain size decrease in the average grain size range from 20 to 0.2 μm. At that, the results of the impedance spectroscopy that provides the opportunity to separate the inputs in this integral conductivity clearly indicate that the grain size conductivity slightly increases during the grain size decrease, while the grain boundary conductivity increases.

Solid electrolytes based on nanosized ceramics are nowadays considered as very perspective materials [109-110]. Conventionally, ceramics with the average grain size less than 100 nm is called nanosized ceramics or nanoceramics [79]. The effect corresponding to the transition from micro to nanosized particles is more complicated.

The authors of [111] investigated the oxygen transport in nanosized dense YSZ using the isotope exchange method. This study was carried out since the results of [92] demonstrate that the amount of oxygen vacations in the grain boundary core is higher than that in the bulk. Thus, one can assume the acceleration of the oxygen ion transport in the grain boundary core along these grain boundaries. At that, there was not found any signifi-

cant increase in the oxygen diffusion along the grain boundaries. Such acceleration was observed by the authors of [111] only for the case of porosity or microcracks presence. A lot of works, see, e.g. [79,112,113], report the significant (~ one or even two orders of magnitude) increase in the grain size conductivity; this fact is usually explained by the Shottky barrier model as being due to the increase in the vacancies amount in the space charge layer. Another explanation is the effect of the partial dopant transition to the surface accompanied by the formation of the structure that is different from the bulk one due to the small grain size. At that, the number of the grain size barriers preventing ion transport increases due to the increase in the grain boundary surface.

Authors of [52] investigated the conductivity of nanosized YSZ with the average grain size of ~ 10 nm with yttrium content in the range from 2 to 12 mol.%. It was shown that the maximal conductivity was registered for tetragonal 3YSZ composition instead of cubic 8YSZ composition for microsized samples. The same yttrium composition (3YSZ) is characterized by the minimal activation energy value of 1.12 eV. Note that phase transition from tetragonal to cubic modification takes place at further yttrium content increase from 3%, at that, the electrolyte conductivity decreases. However, the local maximum of the cubic phase conductivity is still observed at 8% of yttria. All the above effects are considered in regarding for the grain boundary effect. High conductivity of nanosized 3TZP system was shown in [86], the latter paper considers the system using the Shottky barrier model. It is shown that the integral grain boundaries conductivity here is one order of magnitude higher than that in microcrystalline sample of the same composition.

[114] showed that the decrease in the grain size of 3YSZ ceramics down to nanoscale gives an opportunity to decrease the grain boundary resistivity, however, this decrease is rather low – about one order of magnitude in case of bulk nanoceramics.

Note that the conductivity of nanosized thin films is lower than that of microsized thin films, the review [115] demonstrates that two orders of magnitude increase in total conductivity is possible.

The decrease in the grain size of the ceria-based solid solutions leads to the increase in their electronic conductivity. For example the addition of rather small amount of gadolinium oxide (~ 1.5 %, the average particle size of the composite is 7 nm) [116] results in the two orders of magnitude increase in the electronic conductivity. Authors assume that it is due to the fact that doping could not take place in the grains due to their nanosize; all dopant is segregated into the grain boundaries. The plot of the conductivity dependence on the oxygen partial pressure has a slope of -1/6 indicating n-type conductivity. Similar results were shown for individual ceria low-doped by GDC (doping content of 0.2%), [117], further increase in the electronic conductivity with the grain size decrease is reported. At a high dopant content (26%), the conductivity dependence is similar to that obtained for microcrystalline samples [116].

The application of the brick model for nanosized ceramics is impossible [104], primarily due to significant increase of the grain boundary conductivity input that is parallel to current. So, some new approach is necessary to describe the grain conductivity and to consider the results of the impedance measurements. Authors of [112,113,118] suggested so-called n-GCM (nanograin composite model) for ceria and zirconia based systems, this model is based on Maxwell-Wagner/Hashin-Shtrinkman effective medium model. Authors of n-GCM state that the attempt to consider the shape of the grain is the significant modification of the above model. The suggested approach provides the opportunity to compute the electrolyte conductivity along with the permittivities of the grains and grain boundaries. However, there are a number of limitations in the n-GCM model: grain size should be within 10-100 nm, grain/grain boundary structure is considered as two-phase system, at that, each phase is assumed as being homogeneous and isotropic.

The peculiarities in the nanosized ceria conductivity are discussed in [117] both for pure and doped samples. An alternative space-chàrge (Mott-Schottky type) model suggested in [119] is applied here to describe the changes in conductivity behavior during the transition to nanosized grains. This model is based on BLM approach, at that, grain boundaries are subdivided into interfacial core and space charge layer. The charge profile in this layer is described using Mott-Schottky model. The space charge is positive in case of ceria. Using this approach, the authors of [117] considered the shape of impedance dependence plot and to explain the significant increase of the electronic conductivity of ceria through the grain boundaries and its integral increase. Note that the number of factors that should be taken into account significantly increases when the average crystallite size is less than Debye wavelength.

9. THE EFFECT OF GRAIN SIZE ON CERAMICS STRENGTH

In addition to electrochemical properties of solid electrolytes, the mechanical strength of the ceramics should be accounted for at their application in electrochemical devices. This strength is especially important for the fuel cell anodes manufactured from zirconia based ceramics, because such anodes are widely used as a supporting unit for the whole fuel cell [120], this statement is also valid for the case of electrochemical sensors [121]. Complex approach is required to provide the proper value of the ceramics mechanical strength. Factors affecting the mechanical strength of the materials and, in particular, zirconia based ceramics, are considered in [122-124]. Note that the mechanical strength of zirconia based ceramics is much better studied that ceria based ceramics strength. This is due to the fact that ZrO_2-based compositions are widely used as barrier coatings, refractory materials, and implants in dentistry and traumatology. As was mentioned above, nanosized ceramics, including bulk nanosized ceramics, is a point of essential interest for modern applications. For this reason, the effect of the grain size on the mechanical strength of the ceramics will be considered in this section, this consideration will be an important addition to the above given review of the grain size effect of the solid electrolytes conductivity.

There are a lot of zirconia based ceramics compositions possessing high mechanical strength. A number of tetragonal (TZP) modification compositions, cubic ones (SZ), and cubic with some tetragonal additions into the ceramic matrix compositions of the standard ZrO_2–Y_2O_3 system are characterized by rather high mechanical strength. It should be also mentioned that ziconia is sometimes used as an addition increasing the mechanical strength of the wide range of oxide ceramics. However, high mechanical strength coupled with high ionic conductively is typical for 8YSZ and 3YTZP compositions only, see the previous Section.

The dependence of the solid electrolyte mechanical strength on the grains size was registered and averaged in [125] for tetragonal zirconia low-doped by yttria. The existence of some critical grain size (300 nm in case of discussed system) is stated. The significant decrease in the ceramics strength takes place at the grain size higher than this critical value, authors of [125] consider this decrease as being due to significant increase in the content of monoclinic phase and the decrease in matrix ability to withstand destruction of the matrix containing metastable tetragonal modification. At the same time, fracture toughness of YTZP with yttria content from 2 to 5% is independent from the grain size [126] for all compactification approaches.

Authors of [127-128] performed the experimental study of 8YSZ, 9CeSZ, and some triple Y_2O_3-CeO_2-ZrO_2 system compositions at 1000 °C. Note that authors are discussing the size of initial agglomerates instead of the grain size, so, it is rather difficult to compare their results with reported in other works. The significant increase in the ceramics mechanical strength is reported for the investigated compositions at the agglomerate size lower than 1 μm. Generally, strength dependence agree with the above mentioned results obtained for metastable tetragonal zirconia modification, however, the results reported in [127-128] cannot be explained by similar mechanisms. The strength of 8YSZ composition is shown to be higher than that for triple system samples (~450 and ~350 MPa, respectively) for the samples with the average agglomerate size ~ 100 nm. CeSZ shows some extremum on the strength vs agglomerate size dependence with a maximum value corresponding to 100 nm. This maximum can be explained by the change in the cerium ion valence proved by ESCA analysis, probably it is due to the increasing cerium reduction resulting from the increase in the grain surface area. The strength of ceria doped solid solutions is reported to be higher than that for yttria doped samples.

There is some gap in the data on the ceria based ceramics mechanical strength, it is mainly due to its lower strength causing impossibility of wide application in devices and as implants. For example, SDC bending strength is 4.5 times lower than that of YSZ ceramics [129]. However, [130] reported that fracture toughness of 20GDC is quite independent from the grain size, it was measured as ~ 1.5 $MPa{\cdot}m^{1/2}$ for the grain sizes ranging from 0.5 to 9.5 mm. The addition of CoO as a sintering agent also does not lead to some strength vs grain size dependence [131].

It should be also noted that there are a lot problems dealing with dense ceramics manufacturing from nanosized precursor powders, these problems also negatively affect ceramic density [132]. Higher pressure should be applied here, an alternative is hot isostatic pressing. For this reason, the cost of ceramics synthesized using nanosized precursor powders is rather high. Authors of [133] suggested to increase the calcination temperature, however, this complicates the treatment process, in addition,

such a temperature increase may cause grain enlargement and change the ceramics structure.

Summarizing the above consideration, we can state that the decrease in the grain size could result in the ceramics strength increase, however, the use of nanoparticles is complicated and causes some problems at ceramics calcination and treatment, high density could be obtained by using specialized compactification approaches. In addition, the cost of nanoparticle synthesis is higher than the standard ceramic powders production. So, some compromise decisions are necessary to couple the advantages of nanoparticles use with labor/cost effectiveness.

10. CONCLUSIONS

1. Zirconia and ceria based solid solutions could possess high ionic conductivity due to doping mechanism, at that, the input of electronic conductivity is negligible.
2. Approaches used for the precursor powders preparation and ceramics densification procedures greatly affect solid oxide electrolytes structure and transport properties.
3. The use of solid solutions based on triple systems with hafnium, titanium, and some other metal oxide additions provides an opportunity to increase the range of temperature and mechanical stability of the electrochemical devices widening the range of their application.
4. The decrease of the grain size down to nanoscale region could result in the significant decrease in the grain boundary resistivity, however, the integral ceramics conductivity also decreases.
5. The behavior of the ceramics conductivity with the microsized grains could be described using BLM approach, while the nanosized ceramics description requires new approaches, n-GCM model could be used for this task.
6. n-type electronic conductivity prevails over ionic conductivity occurring via doping mechanism in pure and low-doped ceria.
7. The decrease in the grain size results in the increase in the mechanical strength of zirconia based ceramics, however, its manufacturing becomes more complicated.

ACKNOWLEDGEMENTS

This work was supported by the Russian Science Foundation (Research Project 14-29-00199).

REFERENCES

[1] B.C. Steele and A. Heinzel // *Nature* **414** (2001) 345.
[2] N.Q. Minh // *J. Am. Ceram. Soc* **76** (1993) 563.
[3] J.W. Fergus // *J. Pow Sourc.* **162** (2006) 30.
[4] S. Akbar, P. Dutta and C. Lee // *Int. J. Appl. Ceram. Technol*. **3** (2006) 302.
[5] C.C. Chao, C.M. Hsu, Y. Cui and F.B. Prinz // *ACSNano* **5** (2011) 5692.
[6] N. Mahato, A. Gupta and K. Balani // *Nanomaterials and Energy* **1** (2011) 27.
[7] P. Kofstad and T. Norby, *Defects and Transport in Crystalline Solids* (University of Oslo, Oslo, 2007).
[8] M.V. Kravchinskaya, In: *Phase Diagram of systems of Refractory Oxides*, ed. by F. Ya. Galahov (Nauka, Leningrad, 1985), p. 303, In Russian
[9] N.Q. Minh and T. Takahashi, *Science and Technology of Ceramic Fuel Cells* (Elsevier, Amsterdam, 1995).
[10] A.R. West, *Solid State Chemistry and Its Application* (Willey, Chichester, 2014).
[11] V.S. Galkin, V.G. Konakov, A. V. Shorohov and E. N. Solovieva // *Reviews on Advanced Materials Science* **10** (2005) 353.
[12] E.A. Ivanova, V.G. Konakov and E.N. Solovieva // *Rev. Adv. Mater. Sci*. **4** (2003) 41.
[13] Ŕ. Brune, M. Lajavardi, D. Fisler and J. Wagner // *Solid State Ionics* **106** (1998) 89.
[14] V.K. Ivanov, G.P. Kopitsa, S.V. Grigoriev, O.S. Polezhaeva and V.M. Garamus // *Physics of Solids* **52** (2005) 898, In Russian.
[15] W.H. Rhodes // *J. Am. Ceram. Soc*. **64** (1981) 638.
[16] T. Masaki // *J.Am.Ceram.Soc*. **69** (1986) 638.
[17] A.P. Druschitz and J.G. Schroth // *J. Am. Ceram. Soc*. **72** (1989) 1591.
[18] H.V. Atkinson and S. Davies // *Metallurgical and Materials Transactions A* **31A** (2000) 2981.
[19] J.Langer, M.J. Hoffmann and O.Guillon // *J. Am. Ceram. Soc.* **94** (2011) 24.
[20] V. Ivanov, S. Paranin, V. Khrustov, A. Medvedev and A. Shtol'ts // *Key Eng. Mater.* **206** (2002) 377.
[21] U. Anselmi-Tamburini, J.E. Garay and Z.A. Munir // *Scripta Materialia* **54** (2006) 823.
[22] P. Miglioralo and V. Parish // *Appl. Phys. Lett.* **44** (1984) 225.

[23] S. Ekelof // *Eng. Sci and Educ. J*. **10** (2001) 37.
[24] W.L. Fielder, H.E. Kautz, J.S. Fordyce and J. Synger // *J. Electrochem. Soc.* **122** (1975) 528.
[25] Z.B. Stoinov, B.M. Graphov, B. Savova-Stoinova and V.V. Elkin, *Elecrtrochemical Impedance* (Nauka, Moscow, 1991), In Russian.
[26] H. Inaba and H.Tagava // *Solid State Ionics* **83** (1996) 1.
[27] J.E. Bauerle // *J. Phis. Chem. Solids* **30**(1969) 2657.
[28] K.E. Adham and A. Hammou // *Solid State Ionics* **9** (1983) 905.
[29] W. Nernst // *Z. Elektrochem*. **6** (1899) 41.
[30] V.V. Kharton, F.M.B. Marques and A.Atkinson // *Solid State Ionics* **174** (2004) 135.
[31] J.A. Kilner and R.J. Brook // *Solid State Ionics* **6** (1982) 237.
[32] U.Anselmi-Tamburini, F.Maglia, G. Chiodelli, P. Riello and S. Buchella // *Appl. Phys. Lett*. **89** (2006) 163116.
[33] J.A. Dawson and I.Tanaka // *Langmuir* **30** (2014) 10456.
[34] X. Guo and R.Yuan // *Solid State Ionics* **80** (1995) 159.
[35] C. Haering, A. Roosen and H.Schichl // *Solid State Ionics* **176** (2005) 253.
[36] V. Goldschmidt // *Zeit. Krist.* **28** (1987) 1, In German.
[37] *Solid State Chemistry*, ed. by J.A. Kilner in: R.Metselaar, H.J.M. Heijinger and J. Schoonman (Elseiver Science Ltd., Amsterdam, 1982).
[38] T.H. Etsell and S.N. Flengas // *Chemical Reviews* **70** (1970) 339.
[39] O.Yu Kurapova, V.G. Konakov, S.N. Golubev, V.M. Ushakov and I.Yu. Archakov // *Rev. Adv. Mater. Sc.* **32** (2012) 112.
[40] T. Settu // *Ceramics International* **26** (2000) 517.
[41] M. Angeles-Rosas, M. A. Camacho-Lopez and E. Ruiz-Trejo // *Solid State Ionics* **181** (2010) 1349.
[42] S.P.S. Badwall, F.T. Chiacchi, S. Rajedran and J. Drennan // *Solid State Ionics* **109** (1998) 167.
[43] S.P.S. Badwall, F.T. Chiacchi and D. Milosevic // *Solid State Ionics* **136** (2000) 91.
[44] C. Haering, A. Roosen, H. Schichl and M.Schnoller // *Solid State Ionics* **176** (2005) 261.
[45] O. Yamamoto, Y. Arati, Y. Takeda, N. Imanishi, Y. Mizutani, M. Kawai and Y. Nakamura // *Solid State Ionics* **79** (1995) 137.
[46] L.J. Gauckler and K.Sasaki // *Solid State Ionics* **75** (1995) 203.
[47] D.K. Hohnke // *J. Phys. Chem. Solids*. **41** (1980) 777.
[48] B.C.H. Steele // *Solid State Ionics* **129** (2000) 95.
[49] M. Mogensen, N.M. Sammes and G.A. Tompsett // *Solid State Ionics* **129** (2000) 63.
[50] D.R. Ou, T. Mori, F. Ye, M. Takahashi, J.Zou and J. Drennan // *Acta Materialia* **54** (2006) 3737.
[51] M. Mori, T.Abe, H. Itoh, O.Yamamoto, Y.Takeda and T.Kawahara // *Solid State Ionics* **74** (1994) 157.
[52] R. Ramamoorthy, D. Sundararaman and S. Ramasamy // *Solid State Ionics* **123** (1999) 271.
[53] J. Van Herle,T. Horita, T. Kawada, N. Sakai, H. Yokokawa and M. Dokiya // *Solid State Ionics* **86-88** (1996) 1255.
[54] T. Kudo and H. Obayashi // *J. Electrochem. Soc*. **123** (1976) 415.
[55] V. B. Glushkova, M.V. Kravchinskaya, A. K. Kuznetsov and P.A. Tikhonov, *Hafnium Dioxide and Its Compounds with Rare-earth Elements* (Nauka, Leningrad, 1984), In Russian.
[56] C. Wang, M. Zinkevich and F. Aldinger // *J. Amer. Ceramic Soc.* **89** (2006) 3751.
[57] B. Matovic, D. Bucevac, M. Prekajski, V. Maksimovic, D. Gautam, K. Yoshida and T. Yano // *J. of European Ceram. Soc.* **32** (2012) 1971.
[58] C. Lu, J.V. Raitano, S. Khalid, L. Zhang and S. Chan // *Journal of Applied Physics* **103** (2008) 124303.
[59] M.F. Trubelja and V.S. Stubican // *Journal of Amer. Ceram. Soc* **74** (1991) 2489.
[60] M.F. Trubelja and V.S. Stubican // *Journal of Amer. Ceram. Soc* **71** (1988) 662.
[61] E.A. Ivanova, V.G. Konakov and E.N. Solovieva // *Rev. Adv. Mater. Sci.***10** (2005) 357.
[62] T.I. Panova, V.B. Glushkova, A.V. Lapshin and V.P. Popov // *Glass Physics and Chemistry* **29** (2003) 93.
[63] S. Zhuiykov // *Journal Of European Ceram. Soc.* **20** (2000) 967.
[64] W.L. Worell // *Solid State Ionics* **52** (1992) 147.

[65] K. Kobayashi, Y. Kai, S. Yamaguchi, N. Fukatsu, T. Kawashima and Y. Iguchi // *Solid State Ionics* **93** (1997) 193.
[66] S.S. Liou and W.L. Worell // *Appl. Phys*. **49** (1989) 25.
[67] G. Rog and G. Borchardt // *Ceramics International* **22** (1996) 149.
[68] T.H. Kimpton, J. Randle and Drennan // Solid State Ionics **149** (2002) 89.
[69] T. Kawada, N. Sakai, H.Yokoawa and M. Dokiya // *Solid State Ionics* **53-56** (1992) 418.
[70] M.K. Mahapatra, N. Li, A. Verma and P. Singh // *Solid State Ionics* **253** (2013) 223.
[71] Y. Lio and L.E. Lao // *Solid State Ionics* **177** (2006) 159.
[72] A.J.A Winnubst and A.J. Burgraaf // *Mat. Res. Bull* **19** (1984) 613.
[73] X. Guo // *J. Am. Ceram. Soc.* **86** (2003) 1867.
[74] Q. Dong, Z.H. Du, T.S. Zhang, J. Lu, X.C. Song and J. Ma // *International Journal of Hydrogen Energy* **34** (2009) 7903.
[75] T.S. Zhang, J. Ma, L.B. Kong, S.H. Chan, P. Hing and J. Kilner // *Solid State Ionics* **167** (2004) 203.
[76] V.V Zyryanov, N.F. Uvarov, V.A Sadykov, A.S. Ulihin, V.G Kostrovskii, V.P. Ivanov, A.T. Titov and K.S. Paichadze // *Journal of Alloys and Compounds* **483** (2009) 535.
[77]. G.A. Tompsett and N.M. Sammes // *Journal of Amer. Ceram. Soc.* **80** (1997) 3181.
[78] S. Ikeda, O. Sakurai, K. Uematsu, N. Mizutani and M. Kato // *Journal of Materials Science* **20** (1985) 4593.
[79] V. Ivanov, S. Shkerin, A. Lipilin, A. Nikonov, V. Khrustov and Al. Rempel // *Electrochemical Energy* **10** (2010) 3, In Russian.
[80] X. Guo and R. Waser // *Progress in Material Science* **51** (206) 151.
[81] S.P.S. Badwal and S. Rajendran // *Solid State Ionics* **70/71** (1994) 83.
[82] R. Gerhardt and A.S. Nowick // *Journal of Amer. Ceram. Soc.* **69** (1986) 641.
[83] M. Godickemeier, B. Michel, A. Oriukas, P. Bohac, K.Sasaki, L. Gauckler, H. Heinrich, P. Schwander, G. Kostorz, H. Hofmann and O. Frei // *J. Mater. Res.* **9** (1994) 1228.
[84] M.L. Mecartney // *Journal of Amer. Ceram. Soc.* **70** (1987) 54.
[85] E.P. Butler // *J. Microsc.* **140** (1985) 171.
[86] X. Guo and Z. Zhang // *Acta Mat.* **51** (2003) 2539.
[87] X. Guo, C.Q. Tang and R.Z. Yuan // *J. Eur. Ceram. Soc*. **15** (1995) 25.
[88] X. Guo and R.Z. Yuan // *J. Mater. Science Lett.* **14** (1995) 25.
[89] G.M. Christie and F.P.F. van Berkel // *Solid State Ionics* **83** (1996) 17.
[90] A.E. Hugnes and B.A. Sexton // *J. Mater. Sci*. **24** (1989) 1057.
[91] G.S.A.M. Teunissen, A.J.A. Winnubst and A.J. Burggraaf // *J. Mater. Sci.* **29** (1992) 5057.
[92] C.A.J. Fisher and S. Matsuraba // *J. Europ. Ceram. Soc.* **19** (1999) 703.
[93] X. Guo and Y. Ding // *J. Electrochem. Soc.* **151** (2003) J1.
[94] D. Bingham, P.W. Tasker and A.N. Cormack // *Philos. Mag. A* **60** (1989) 1.
[95] M. Aoki, Y. Chiang, I. Kosacki, L. J. Lee, H. Tuller and Y. Liu // *J. Amer. Ceram. Soc.* **79** (1996) 1169.
[96] M. Filal, C. Petot, M. Mokchah, C. Chateau and J.L. Carpentier // *Solid State Ionics* **80** (1995) 27.
[97] M.J. Verkerk, A.J.A. Winnubst and A.J. Burgraaf // *J. Mater. Sci.* **17** (1982) 3113.
[98] D.Z. de Florio and R. Muccillo // *Solid State Ionics* **123** (1999) 301.
[99] D. Kim, P. Cho, J. Lee, D. Kim and S.B. Lee // *Solid State Ionics* **177** (2006) 2125.
[100] J. Lee, T. Mori, J. Li, T. Ikegami, M. Komatsu and H. Haneda // *J. Electrochem. Soc.* **147** (2000) 2822.
[101] A. Rizea, C. Petot, G. Petot-Ervas, M.J. Graham and G.I. Sproule // *Ionics* **7** (2001) 72.
[102] N.M. Beekmans and L. Heyne // *Electrochim. Acta* **21** (1976) 23.
[103] T. van Dijk and A.J. Burgraaf // *Phys. Stat. Solidi A*. **63** (1981) 229.
[104] N.J. Kidner, N.H. Perry and T.O. Mason // *J. Amer. Ceram. Soc.* **91** (2008) 1733.
[105] H. Nafe // *Solid State Ionics* **13** (1984) 255.
[106] J. Khare, M.P. Joshi, S. Satapathi, H. Srivastava and L.M. Kukreja // *Ceram. Int.* **40** (2014) 14677.
[107] A. Heel, A. Vital, P. Holtappels and T. Graule // *J. Electroceram*. **22** (2009) 40.
[108] A.I. Ioffe, M.V. Inozemtsev, A.S. Lipilin, M.V. Perfilev and S.V. Karpachov // *Phys. Stat. Sol*. **30** (1975) 87.

[109] H.L. Tuller // *Solid State Ionics* **131** (2000) 143.
[110] J. Schoonman // *Solid State Ionics* **135** (2000) 5.
[111] R.A. De Souza, M.J. Pietrowski, U. Anselmi-Tamburini, S. Kim, Z.A. Munir and M. Martin // *Phys. Chem Chem Phys.* **10** (2008) 2067.
[112] N.H. Perry, S. Kim and T.O.Mason // *J. Mater. Sci.* **43** (2008) 4684.
[113] N.H. Perry and T.O. Mason // *Solid State Ionics* **181** (2010) 276.
[114] X. Guo // *Scripta Mat*. **65** (2011) 96.
[115] S. Hui, J. Roller, S. Yick, X. Zhang, C. Deces-Petit, Y. Xie, R. Maric and D. Ghosh. // *J. Pow. Sources* **172** (2007) 493.
[116] Y.M. Chiang, E.B. Lavik and D.A. Bloom // *Nanostructured Mater.* **9** (1997) 633.
[117] S. Kim and J. Maier // *J. Electrochem. Soc*. **149** (2002) J73.
[118] T.C.Yeh, N.H. Perry and T.O. Mason // *J. Am. Ceram. Soc*. **94** (2011) 1073.
[119] A. Tshope, E. Sommer and R. Birringer // *Solid State Ionics* **139** (2001) 255.
[120] S.C. Singhal and K. Kendal, *High Temperature Solid Oxide Fuel Cells: Fundamentals, Design and Applications* (Elsevier, Oxford, 2003).
[121] S. Zhuiykov, *Electrochemistry of Zirconia Gas Sensors* (CRC Press, Boca Raton, 2008).
[122] I. Birkby and R. Stevens // *Key Engineering Materials* **122-124** (1996) 527.
[123] J.R.Kelly and I. Denry // *Dental Materials* **24** (2008) 289.
[124] P. Bosh and J.C. Niepce, C*eramic Materials: Processing, Properties and Application* (Antony Rowe ltd., Chippenham, 2007).
[125] T.K. Gupta, F.F. Lange and J.H. Bechtold // *J. Mater. Sci.* **13** (1978) 1464.
[126] T. Masaki // *J. Amer. Chem.Soc*. **69** (1986) 638.
[127] V.G. Konakov, S. Seal, E.N. Solovieva, M.M.Pivovarov, S.N. Golubev and A.V. Shorochov // *Rev. Adv. Mater. Sci*. **13** (2006) 71.
[128] V.G. Konakov, S. Seal, E.N. Solovieva, D.A. Ivanov-Pavlov, M.M.Pivovarov, S.N. Golubev and A.V. Shorochov // *Rev. Adv. Mater. Sci*. **16** (2007) 96.
[129] J.W.Adams, R. Ruh and K.S. Mazdiyasni // *J. Amer. Ceram. Soc*. **80** (1997) 903.
[130] T.S. Zhang, J. Ma, L.B. Kong, P. Hing and J. A. Kilner // *Solid State Ionics* **167** (2004) 191.
[131] C. Kleinlogel and L.J. Gauckler // *Solid State Ionics* **135** (2000) 567.
[132] M. Cain and R. Morell // *Appl. Organometallic Chem.* **15** (2001) 321.
[133] J. Ma, T.S. Zhang, L.B. Kong, P. Hing, Y.J. Leng and S.H. Chan // *J. Eur. Ceram. Soc.* **24** (2004) 2641.
[134] L.H. Ahrens // *Geochimica and Cosmochimica Acta* **2** (1952) 155.